Application of Homogeneous Transformation Matrices to the Simulation of VLP Systems

Technical Report · November 2017

DOI: 10.13140/RG.2.2.31780.58248

1 author:

Pedro Fonseca
University of Aveiro
43 PUBLICATIONS **293** CITATIONS

SEE PROFILE

Application of Homogeneous Transformation Matrices to the simulation of VLP systems

Pedro Fonseca

November 21, 2017

Abstract

In robotics, Homogeneous Transformation Matrices (HTM) have been used as a tool for describing both the position and orientation of an object and, in particular, of a robot or a robot component [1]. In this work, we propose an approach to the simulation of a Visible Light Positioning system where HTMs are used to represent the position of the different system elements, both for the optical component, comprising the emitters and receivers, and for the robotic devices.

1 Introduction

Although widely used in open-air, outdoor applications for localization services, Global Positioning System (GPS) is unable to provide location inside buildings [2]. As such, several alternative methods have risen for Indoor Positioning Systems. Among these methods, one can mention those based on infrared (IR), ultrasound, radio frequency (RF) and, more recently, Visible Light Positioning (VLP). Use of VLP has been driven by the spread usage of LED based lighting systems. LED illumination presents several advantages such as high luminosity, low power consumption and low heat generation [3], which together with the possibility of modulating light makes every luminary a potential data broadcaster.

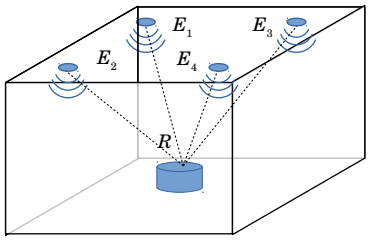

Figure 1: Principle of visible light positioning.

The principle of VLP usually lies on the computation by the positioning sensor of its position relative to a fixed set of light emitters, the position of these emitters being previously known or somehow provided to the sensor. By computing the position relative to a fixed frame of light emitters whose absolute

position is known, the absolute position of the mobile agent can be immediately derived. This is presented in figure 1, showing four emitters, E_1 to E_4, that are totally or partially detected by the receiver R. The characteristics of the signal received from each of these emitters (amplitude, direction, encoded data, ...) are used in an algorithm that computes the receiver's location relative to the set of emitters. As such, VLP depends on the existence of an Optical Wireless Communication (OWC) channel between each emitter and each receiver. Modelling this OWC channel is therefore required to simulate the behaviour of a VLP system.

2 Channel model

In this section, we will address the definition of a model for the optical channel between the emitter and the receiver. This model follows the works of Gfeller and Bapst [4] and Kahn and Barry [5].

Two assumptions are introduced about the light emitter and receiver system. The first assumption is that the angular distribution of optical power in the light source is modelled by a Lambertian model, following [4] and [6]. This is a model suitable to represent the optical power radiated by a planar LED [7].

Assumption 1 *The light sources are represented by a Lambertian model.*

The second assumption is the optical power in light reflections and diffuse components can be neglected, when compared to the optical power in the line-of-sight (LOS) channel. This follows the approach in previous works [8, 9, 10]. According to [11], although the received power from reflections can be significant in infra-red lighting, in the case of visible light, the power coming from reflections is smaller and thus can be disregarded.

Assumption 2 *The optical power originating from reflections is negligible, when compared to the power in direct line-of-sight channel.*

In a LOS channel, with no reflections, the average received power is $P = H^0(0)P_t$, where P_t is the average transmitted optical power and $H^0(0)$ is the d.c. channel gain; the superscript 0 accounts for the number of reflections.

A LOS channel can be represented as in figure 2. Emitter E and receiver R are at a distance d apart. E emits along a preferred axis; the *irradiance angle* is defined as the angle ϕ between the emitter axis and the line connecting E and R. The light beam arrives at the receiver with an angle of incidence ψ, defined as the angle between the line connecting E and R and the normal of the detector surface.

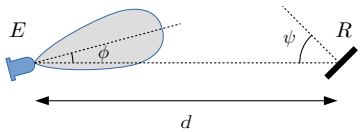

Figure 2: Line-of-sight (LOS) optical channel

The d.c. gain for a generalized Lambertian emitter is given by [5]:

$$H_{ER}^0(0) = \begin{cases} \frac{m+1}{2\pi} \cos^m(\phi) \cos(\psi) \frac{A_r}{d^2} T_s(\psi) g(\psi), & 0 \leq \psi \leq \Psi_c \\ 0, & \psi > \Psi_c \end{cases} \tag{1}$$

where ϕ and ψ are respectively the irradiance and the incidence angle, defined as above, d is the distance from E to R, m is the Lambertian index number, A_r is the area of the the detecting surface, T_s is the receiver filter gain, g is the concentrator gain in the receiver and Ψ_c is the half field of view (HFOV) angle [12].

For the case of an idealized non-imaging concentrator, g is defined by:

$$g(\psi) = \begin{cases} \frac{n^2}{\sin^2 \Psi_c}, & 0 \leq \psi \leq \Psi_c \\ 0, & \psi > \Psi_c \end{cases} \tag{2}$$

where n is the internal refractive index of the receiver. Eq. (2) can be rewritten as:

$$g(\psi) = \frac{n^2}{\sin^2 \Psi_c} \cdot v(\psi \leq \Psi_c) \tag{3}$$

where $v()$ is the *veracity function*, returning 1 if the argument is true and 0 otherwise. The form in (3) is preferred, as it is provides faster computer implementation.

3 Geometric model

We will now consider the representation of the emitter and receiver as geometric entities in a three-dimensional space. Consider figure 3, where E is the emitter, R the receiver and $\mathbf{O}$ is the origin of the coordinate system. $\mathbf{p}_E$ and $\mathbf{p}_R$ are the position vectors of the emitter and receiver, respectively; $\mathbf{n}_E$ is the unit vector in the direction of the emitter main axis and $\mathbf{n}_R$ is the unit vector of the normal to the receiver's detecting surface. As above, ϕ and ψ are, respectively, the irradiance and incidence angles.

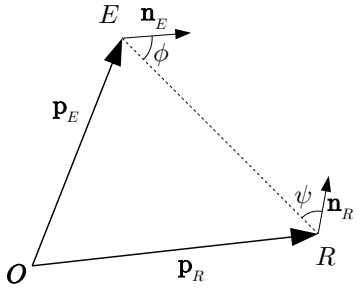

Figure 3: Emitter and receiver

A reference frame, represented by a HTM, is associated to each emitter and receiver: the origin of the reference frame is place at the element position and the z-axis of the reference frame is aligned with the element main axis, pointing to the emission direction, in the case of emitters, and in the receiving direction, for the receivers. As the model stands now, light polarization is not considered.

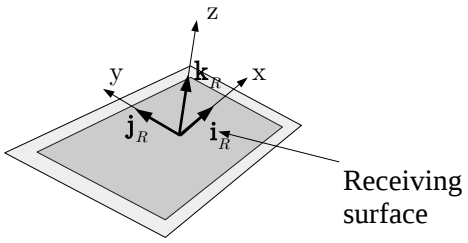

Figure 4: Reference frame associated to a receiver.

As such, the position of both x and y axes is irrelevant, as long as they define a reference frame, together with the z axis. In other words, any frame created by the rotation of the frame in figure 4 around the z axis would be equally acceptable.

If we consider the emitter axis to be aligned with the respective frame z axis, then $\mathbf{n}_E = \mathbf{k}_E$. In the same way,

$$\mathbf{HTM}_R = \begin{bmatrix} \mathbf{i}_R & \mathbf{j}_R & \mathbf{k}_R & \mathbf{p}_R \\ 0 & 0 & 0 & 1 \end{bmatrix}$$

and $\mathbf{n}_R = \mathbf{k}_R$.

The computation of the channel gain from E to R requires the computation of the cosine of both ϕ and ψ. Defining $\mathbf{D}_{ER} = \mathbf{p}_R - \mathbf{p}_E$ as the vector pointing from E to R and $d = \|\mathbf{D}_{ER}\|$ as the distance from E to R, it is immediate that:

$$\cos\phi = \frac{\mathbf{n}_E \cdot \mathbf{D}_{ER}}{d} \tag{4}$$

where $\cdot$ stands for vector dot product. Defining $\mathbf{u}_{ER}$ as the unit vector in the direction from E to R, (4) reduces to

$$\cos\phi = \mathbf{n}_E \cdot \mathbf{u}_{ER} \tag{5}$$

Similarly:

$$\cos\psi = \mathbf{n}_R \cdot (-\mathbf{u}_{ER}) \tag{6}$$

The homogeneous transformation matrices representing the position and orientation of the emitter and receiver provide, directly, the values for the computations above. Considering the $\mathbf{HTM}_E$, the matrix that defines the position and orientation of the emitter:

$$\mathbf{HTM}_E = \begin{bmatrix} \mathbf{i}_E & \mathbf{j}_E & \mathbf{k}_E & \mathbf{p}_E \\ 0 & 0 & 0 & 1 \end{bmatrix}$$

$\mathbf{i}_E$, $\mathbf{j}_E$ and $\mathbf{k}_E$ define the emitter's frame and correspond to the coordinates of the unit vectors for the x, y and z axis of the emitter frame, respectively, expressed in coordinates of the base frame. $\mathbf{p}_E$ can be immediately retrieved from $\mathbf{HTM}_E$.

In this case, (1) can be expressed as:

$$H_{ER}^0(0) = \begin{cases} \frac{m+1}{2\pi} A_r T_s(\psi) g(\psi) \frac{(\mathbf{n}_E \cdot \mathbf{u}_{ER})^m (\mathbf{n}_R \cdot (-\mathbf{u}_{ER}))}{d^2}, & 0 \leq \psi \leq \Psi_c \\ 0, & \psi > \Psi_c \end{cases} \tag{7}$$

4 Systems with multiple emitters and receivers

Consider now the situation where a set of n emitters $\mathbf{E} = \{E_1, E_2, \ldots, E_n\}$ transmits to a set of m receivers $\mathbf{R} = \{R_1, R_2, \ldots, R_m\}$. The position and orientation of each emitter and receiver is known, as well as the parameters that describe each of these. Defining $\mathbf{p}_t = [p_{t,1}, p_{t,2}, \ldots, p_{t,n}]^{\mathrm{T}}$ as a $n \times 1$ column vector where $p_{t,j}$ is the power radiated by the j-th emitter and $\mathbf{p}_r = [p_{r,1}, p_{r,2}, \ldots, p_{r,n}]^{\mathrm{T}}$ a $m \times 1$ column vector with the power received by each photo-detector, their relationship can be expressed as

$$\mathbf{p}_r = \mathbf{H}\ \mathbf{p}_t \tag{8}$$

where $\mathbf{H}$ is a $m \times n$ matrix, where each h_{ij} corresponds to the channel gain from the j-th emitter to the i-th receiver:

$$h_{ij} = \frac{m_j + 1}{2\pi} A_{r,i} T_{s,i} g_{ij} \frac{(\mathbf{n}_{E_j} \cdot \mathbf{u}_{\mathbf{j},\mathbf{i}})^{m_j} (\mathbf{n}_{R_i} \cdot \mathbf{u}_{\mathbf{i},\mathbf{j}})}{d_{i,j}^2}\ v(\psi_{i,j} \leq \Psi_{c,i}) \tag{9}$$

where, to each symbol, the subscript i or j was added, if the symbol refers to the receiver or emitter, respectively (*e.g.*, $\Psi_{c,i}$ is the HFOV angle for the i-th receiver). For the terms relating to the emitter and receiver, both subscripts were added: $\psi_{i,j}$ is the incidence angle considering the j-th emitter to the i-th receiver. It is possible to distinguish in (9) a set of terms that depend only on the emitter or receiver and another part that depends on the spatial location and orientation of both the emitters and receivers.

The value of the idealized non-imaging concentrator function g_{ij} depends on both the emitter j and receiver i; more specifically, it depends on the incidence angle ψ, which in turn depends on the position of the j-th emitter relative to the i-th receiver. The computation of (3) still requires to explicitly compute the angle ψ_{ij}. By taking in consideration that i) $\cos(\psi_{ij})$ can be computed directly from the data in the HTMs of the emitter and receiver using simple algebraic manipulation, ii) $\psi_{ij} \in [0, \pi/2]$ and iii) the cosine function is monotonically decreasing in that interval, we get:

$$\psi_{ij} \leq \Psi_{c,i} \Leftrightarrow \cos(\psi_{ij}) \geq \cos(\Psi_{c,i}) \quad 0 \leq \psi_{ij}, \Psi_{c,i} \leq \pi/2 \tag{10}$$

g_{ij} can now be expressed as:

$$g_{ij}(\psi_{ij}) = \frac{n_i^2}{\sin^2(\Psi_{c,i})}\ v\left(\mathbf{n}_{R_i} \cdot \mathbf{u}_{ij} \geq \cos(\Psi_{c,i})\right) \tag{11}$$

where $v()$ is the veracity function, defined as above.

Each element of $\mathbf{H}$ can now be expressed as

$$\begin{aligned} h_{ij} &= \frac{m_j + 1}{2\pi} A_{r,i} T_{s,i} \frac{n_i^2}{\sin^2(\Psi_{c,i})} \times \\ &\quad \times v\left(\mathbf{n}_{R_i} \cdot \mathbf{u}_{ij} \geq \cos(\Psi_{c,i})\right) \frac{(\mathbf{n}_{E_j} \cdot \mathbf{u}_{\mathbf{j},\mathbf{i}})^{m_j} (\mathbf{n}_{R_i} \cdot \mathbf{u}_{\mathbf{i},\mathbf{j}})}{d_{i,j}^2} \end{aligned} \tag{12}$$

$$= a_i\ b_j\ f_{ij} \tag{13}$$

with a_i accounting for the terms depending on the i-th receiver, b_j comprising the terms depending on the j-th emitter only and f_{ij} accounting for the terms that depend on both the emitter and receiver and that are related to the geometry of the spatial distribution of the emitters and the receivers.

By expressing h_{ij} as in (13) it is possible to factorize $\mathbf{H}$ in the form

$$\mathbf{H} = \mathbf{A}\ \mathbf{F}\ \mathbf{B} \tag{14}$$

and (8) can be expressed as:

$$\mathbf{p}_r = \mathbf{A}\ \mathbf{F}\ \mathbf{B}\ \mathbf{p}_t \tag{15}$$

$\mathbf{A}$ is a $m \times m$ diagonal matrix containing the terms related to the receiver, defined by:

$$a_{ij} = A_{r,i}\ T_{s,i}\ \frac{n_i^2}{\sin^2(\Psi_{c,i})}\ \delta_{ij} \tag{16}$$

where δ_{ij} is the Kronecker delta. $\mathbf{B}$ is a $n \times n$ diagonal matrix with the terms describing the emitter:

$$b_{ij} = \frac{m_j + 1}{2\pi}\ \delta_{ij} \tag{17}$$

and $\mathbf{F}$ is a $m \times n$ matrix with the terms related to the spatial distribution of emitters and receivers:

$$\begin{aligned} f_{ij} &= v\left(\mathbf{n}_{R_i} \cdot \mathbf{u}_{ij} \geq \cos(\Psi_{c,i})\right) \frac{(\mathbf{n}_{E_j} \cdot \mathbf{u}_{\mathbf{j},\mathbf{i}})^{m_j} (\mathbf{n}_{R_i} \cdot \mathbf{u}_{\mathbf{i},\mathbf{j}})}{d_{i,j}^2} \\ &= v\left(\mathbf{n}_{R_i} \cdot \mathbf{u}_{ij} \geq \cos(\Psi_{c,i})\right) \frac{(\mathbf{n}_{E_j} \cdot \mathbf{u}_{\mathbf{j},\mathbf{i}})^{m_j} (\mathbf{n}_{R_i} \cdot \mathbf{u}_{\mathbf{i},\mathbf{j}})}{(\mathbf{p}_{E_j} - \mathbf{p}_{R_i}) \cdot (\mathbf{p}_{E_j} - \mathbf{p}_{R_i})} \end{aligned} \tag{18}$$

The matrices $\mathbf{A}$ and $\mathbf{B}$ are constant for a given set of emitters and receivers. If the position of the emitters or receivers changes, only the matrix $\mathbf{F}$ needs to be recalculated.

5 Noise model

The model defined above for the system of emitters and receivers allows us to compute the optical power impinging on the receiver photo-detectors. To use this information in a practical application, such as estimating the sensor location, an electrical signal must be extracted from the photo-detector. In this section, we will derive the model for the conversion from optical power to an electric quantity, including the noise generated in the process.

5.1 Signal sources

The incidence of an optical power of magnitude p_r on a photo-detector produces an electric current, the photo-current i_p. The average value of this current is given by [7]

$$\langle i_p \rangle = \frac{\eta_{qe} q \lambda p_r}{hc} = R p_r \tag{19}$$

where

$$R = \frac{\eta_{qe} q \lambda}{hc} \tag{20}$$

is the *responsivity* of the photo-detector.

In the case of IM-DD (Intensity Modulation - Direct Detection), the generated current is directly proportional to the instantaneous received power:

$$i_p(t) = RMp_r(t) \tag{21}$$

where $p_r(t)$ represents the instantaneous value of received optical power and M is a multiplicative factor. In the following, we will consider the case of a PIN photo-diode, where $M = 1$.

5.2 Noise sources

According to Ghassemlooy *et al* [7], in an optical communication system, there are two main sources of noise in the signal at the receiver: shot noise from the received photo-current and noise from the receiver electronics.

To compute the noise generated in the receiver electronics, we consider that the photo-diode signal is processed using a transimpedance amplifier (figure 5). The output voltage v_o, considering a photo-current i_p, is:

$$v_o = R_f \, i_p \tag{22}$$

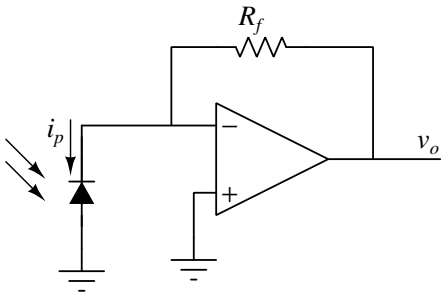

Figure 5: Transimpedance amplifier circuit.

Figure 6 presents a model for analysing the transimpedance amplifier, together with the noise sources that occur in the circuit, represented by current or voltage sources and identified with the subscript n. i_p is, as before, the photo-diode current. The main source of noise in the photo-diode is shot noise, modelled by the current $i_{n,sh}$. The noise sources related to the electronic circuit are the voltage and current sources that represent noise generated in the operational amplifier, $v_{n,op}$ and $i_{n,op}$, and the thermal noise generated in the feedback resistor, $v_{n,th}$. C_p and R_p represent the resistance and capacitance of the photo-diode model.

Shot noise is modelled as a Gaussian noise with variance:

$$\sigma^2_{\mathrm{n,sh}} = 2q\langle i_p \rangle B \tag{23}$$

where q is the electron charge and B the bandwidth of the circuit following the photo-detector.

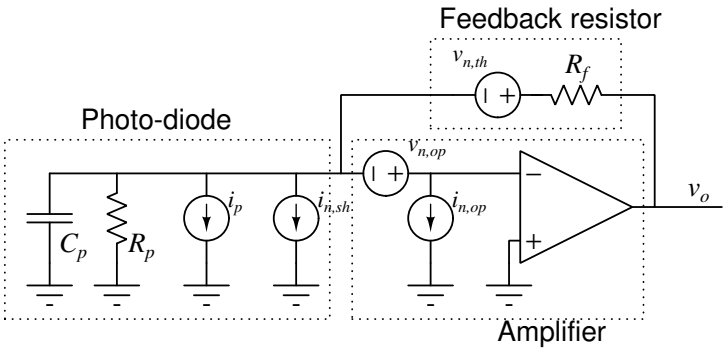

Figure 6: Equivalent circuit with noise sources.

Thermal noise in the feedback resistor R_f is given by:

$$\sigma^2_{n,th} = 4k_B\Theta R_f B \tag{24}$$

where k_B is the Boltzmann's constant and Θ is the thermodynamic temperature.

All the noise sources are considered to be uncorrelated random variables, with mean value zero. Shot and thermal noise are gaussian, white noise with zero mean.

Noise in operational amplifiers presents a white noise component superposed to a $1/f$ component. Figure 7 presents the power spectral density (PSD) of OPA657, an operational amplifier suitable for photo-diode current amplification [13]. The effect of a $1/f$ component is clearly visible at low frequencies while white noise dominates at higher frequencies, the corner frequency being located at approximately 1 kHz. For the current noise, this op-amp presents a power spectral density that is independent of the frequency.

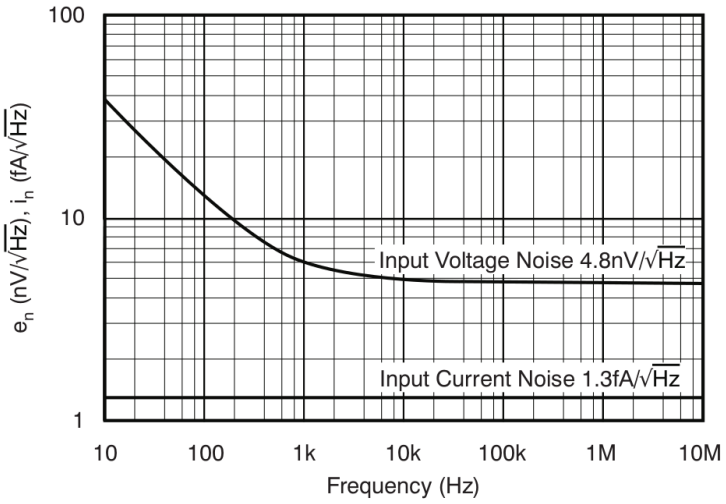

Figure 7: OPA657 power spectral density.

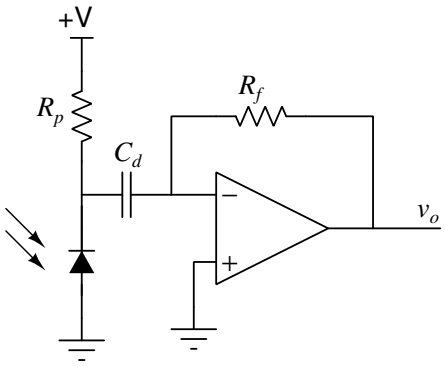

Figure 8: Photo-diode amplifier circuit with DC rejection.

For the general case, noise contribution from $v_{n,op}$ and $i_{n,op}$ will be given by:

$$\sigma^2_{i|n,op} = \int_B S_i^2(f)df \tag{25}$$

$$\sigma^2_{v|n,op} = \int_B S_v^2(f)df \tag{26}$$

where S_i and S_v and the power spectral density for the noise current and voltage sources in the operational amplifier.

The noise PSD in figure 7 allows us to introduce some assumptions that will simplify the estimation of the contribution from $v_{n,op}$ and $i_{n,op}$ to circuit noise. As the incoming light is modulated, the signal conditioning chain will very likely include a filter for DC rejection of the photo-current signal. This corresponds to the circuit in figure 8 and the objective is to reject DC and low frequency components that correspond to undesired interferences, such as sunlight. The introduction of a band pass filter downstream in the signal processing chain will not degrade the signal and it will reject low frequency $1/f$ noise. Moreover, the corner frequency in the noise PSD is usually located in the range up to 100 Hz in general purpose amplifiers, reaching the hundreds of Hertz or even 1 to 2 kHz in high speed amplifiers [14]; the example in figure 7 refers to an amplifier with a 1.6 GHz gain-bandwidth product. One can expect that an amplifier with a high value for the corner frequency will be used in amplifying a signal with high frequency components, being thus reasonable that rejecting signal components in the kHz range will not degrade the signal quality. As such, we will consider both noise sources in the operational amplifier to have a constant PSD in the optical signal modulating frequencies range. In this case, the noise contribution from the sources related to the operational amplifier can be simplified to:

$$\sigma^2_{i|n,op} = S_i^2 B \tag{27}$$

$$\sigma^2_{v|n,op} = S_v^2 B \tag{28}$$

5.3 Output referred noise

Having identified and quantified noise sources of noise, the following step is to compute the total noise in the circuit. Figure 9 presents the equivalent circuit, when all noise sources are projected to the input as current sources.

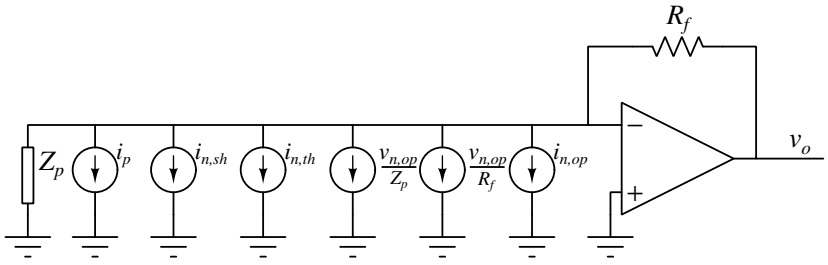

Figure 9: Equivalent noise sources projected to the input.

The equivalent noise current referred to the input will be the sum of all noise currents. All these noise sources are considered to be uncorrelated random variables, except for the two current sources that depend on $v_{n,op}$. The variance of the equivalent noise current, and thus the noise power at the input, is given by:

$$\begin{aligned}\sigma^2_{n,input} &= \sigma^2_{n,sh} + \sigma^2_{n,th} + \sigma^2_{v|n,op}\left|\frac{1}{Z_p} + \frac{1}{R_f}\right|^2 + \sigma^2_{i|n,op} \\ &= \left[2qi_p + \frac{4k_B\Theta}{R_f} + S_v^2\left|\frac{Z_p + R_f}{Z_p R_f}\right|^2 + S_i^2\right] B \end{aligned} \tag{29}$$

The signal at the amplifier output will be a voltage v_o with mean value μ_{v_o} and variance $\sigma^2_{v_o}$:

$$\mu_{v_o} = R_f \cdot i_p \tag{30}$$

$$\begin{aligned}\sigma^2_{v_o} &= R_f^2 \cdot \sigma^2_{n,input} \\ &= \left[\left(2qi_p + S_i^2\right) R_f^2 + 4k_B\Theta R_f + S_v^2\left|1 + \frac{R_f}{Z_p}\right|^2\right] B \end{aligned} \tag{31}$$

5.4 Noise computation and model representation

A key aspect in the behaviour will the Signal to Noise Ratio (SNR) in the received optical signal. The optical signal sent by emitters is modulated in amplitude, using IM-DD, and it is comprised of an information carrier of null mean superposed on a constant amplitude signal, the ratio of the amplitude of the varying component to the amplitude of the constant base signal being the modulation depth. Among other things, the modulating signal will be used by the VLP algorithm to identify the signal source.

The shot noise component in the detected signal depends on the average value of the photo-diode current, i_p. This corresponds to the contribution of the constant amplitude component of the optical signal, as the modulating signal has null mean. As such, when computing the SNR, the signal power will depend

on the amplitude of the modulating signal and noise will have a shot noise component that depends on the DC component. Furthermore, when signal from multiple emitters impinge on a receiver, the DC components are added and all received signals contribute to the shot noise component.

To model these conditions, the emitters optical power $\mathbf{P_t}$ will represented by a $(n \times n+1)$ matrix in the form

$$\mathbf{P_t} = [\mathbf{p_b} \,|\, \mathbf{P_s}] = \begin{bmatrix} p_{b,1} & p_{s,1} & & & \\ p_{b,2} & & p_{s,2} & & \\ \vdots & & & \ddots & \\ p_{b,n} & & & & p_{s,n} \end{bmatrix} \tag{32}$$

where $p_{b,i}$ is the power associated to the base (DC) component in the i-th emitter and $P_{s,ii}$ is the power associated to the signal component in the same emitter. $\mathbf{p_b}$ is a column vector with n elements and $\mathbf{P_s}$ is a $(n \times n)$ diagonal matrix (all $p_{s,ij} = 0$, for $i \neq j$).

Under this formulation, the result of (8) becomes:

$$\begin{aligned} \mathbf{P_r} &= \mathbf{H}\,\mathbf{P_t} \\ &= [\mathbf{n_b}|\mathbf{Q}] \end{aligned} \tag{33}$$

$\mathbf{n_b} = \mathbf{H}\,\mathbf{p_b}$ is a $(n \times 1)$ vector with the power associated to the constant optical signal component, where $n_{b,i} = h_{i1}p_{b,1} + \cdots + h_{in}p_{b,n}$ is the power associated to the DC component in receiver i generated by the n emitters, and $\mathbf{Q} = \mathbf{H}\,\mathbf{P_s}$ is a $(m \times n)$ matrix containing the power associated to the signal components, where $q_{ij} = h_{ij}\,p_{s,j}$ represents the optical power detected in receiver i originating from emitter j.

The signal detected at the amplifier output is given by a matrix $\mathbf{Y}$ where each element y_{ij} represents the signal received in receiver i from emitter j:

$$\mathbf{Y} = \mathrm{diag}(\mathbf{z})\,\mathbf{R}\,\mathbf{Q} \tag{34}$$

$\mathbf{z}$ is a column vector where the i-th element z_i is the feedback resistor in the amplifier circuit of the i-th receiver and $\mathbf{R}$ is a $(m \times m)$ diagonal matrix where r_{ii} is responsivity of the i-th receiver.

Noise affecting the m receiver circuits outputs has a power given by the vector ν:

$$\nu = \left[\mathbf{z}^{\circ 2} \odot \left(2q\,\mathbf{R}\,\mathbf{n_b} + \mathbf{s_i}^{\circ 2}\right) + 4k_B\Theta\,\mathbf{z} + \left(|\mathbf{1}_m + \mathbf{z} \oslash \mathbf{z_p}| \odot \mathbf{s_v}\right)^{\circ 2}\right] B \tag{35}$$

where $\mathbf{s_i}$ and $\mathbf{s_v}$ are two column vectors with the current and voltage PSD of the m amplifiers, $\mathbf{1_m}$ is a column vector of ones of dimension m, $\mathbf{z_p}$ is a column vector where $z_{p,i}$ is the equivalent impedance of the diode in the i-th receiver, $\odot$ is the Hadamard product, $\oslash$ the Hadamard division and $^{\circ 2}$ denotes the Hadamard power. [1].

The output of the m receivers can be represented by a matrix of random variables $\mathbf{Y}^*$ where each element y^*_{ij} follows a normal distribution:

$$y^*_{ij} = \mathcal{N}\left(y_{ij}, \nu_i\right) \tag{36}$$

[1] Hadamard product, division and power correspond in Matlab to the element-wise operations and are represented by the operators `.*`, `./` and `.^`, respectively.

Most computational systems provide a means of generating random variables with normal distribution, namely following a normalized Gaussian distribution with $\mu = 0$ and $\sigma = 1$. In this case, having a matrix $\mathbf{T}$ of independent random variables following a normalized Gaussian distribution and with the same size of $\mathbf{Y}$, $\mathbf{Y}^*$ can be computed by:

$$\mathbf{Y}^* = \mathbf{Y} + \left(\nu^{\circ(1/2)} \cdot \mathbf{1}_{\mathbf{n}}^T\right) \odot \mathbf{T} \tag{37}$$

The Signal-to-Noise Ratio for every emitter-receiver pair is given by the matrix $\mathbf{S}$:

$$\mathbf{S} = \left(\mathbf{Y}^{\circ 2}\right) \oslash \left(\nu \cdot \mathbf{1}_{\mathbf{n}}^T\right) \tag{38}$$

Each element s_{ij} contains the Signal-to-Noise Ratio in the transmission from the j-th emitter to the i-th receiver.

6 VLP system simulation

In the case of a Visible Light Position system, the sensor will be defined as a geometric arrangement of a set of m receivers. We consider that the sensor is rigid, meaning that the relative position of the photo-detectors in the sensor does not change. This means that pose of every detector is uniquely determined by the sensor position. An example of a possible sensor arrangement is presented in figure 10. In this case, the receivers, photo-diodes, are placed in a hemispherical surface, at the intersection of meridian and parallel lines.

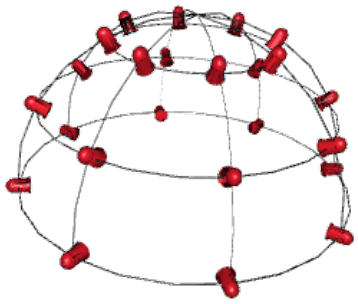

Figure 10: Sensor arrangement.

In geometrical terms, a reference frame is assigned to the sensor, defining the sensor pose in a 3D space, and the relative position and orientation of each receiver w.r.t. the sensor reference frame is known. Let us define $\mathbf{L_s}$ as the reference frame representing the sensor pose (location and orientation in 3D space). The geometrical arrangement of the location sensor is defined by the pose of each photo-detector w.r.t. the sensor reference frame.

The arrangement in figure 1 allows us to introduce some assumptions about the VLP system. In this case, the emitters are fixed (they do not change in position or orientation) and we will assume that their optical characteristics, including emitted power, are constant. In the receiver side, we will also consider the receiver optical characteristics to be constant.

As the receivers are photo-detectors arranged in a sensor, we will also introduce the assumption that the sensor configuration, *i.e.*, the position of the photo-detectors relative to the sensors reference frame, does not change.

Assumption 3 *The emitters position and orientation do not change.*

Assumption 4 *The sensor is rigid; the relative position of the photo-detectors in the sensor does not change.*

Equation (15) establishes the relation between the emitted power at the light sources and the power detected at the receivers. In this equation, the matrix $\mathbf{F}$ contains the information about the system geometry: the pose (location and orientation) of all emitters and receivers, as well as the field-of-view of the receivers. Introducing assumptions 3 and 4 makes $\mathbf{F}$ implicitely dependent on the sensor pose, $\mathbf{L_s}$, as this determines the pose of every receiver. In this sense, we can say that, under assumptions 3 and 4, that $\mathbf{p_r}$, the power detected at the receivers, is a function of $\mathbf{L_s}$, the sensor position.

$$\mathbf{p_r} = f(\mathbf{L_s}) \tag{39}$$

In this case, the problem of Visible Light Positioning can be defined as identifying f^{-1}, the inverse of f in (39), in order to compute the sensor position, given the power detected at the receivers.

$$\mathbf{L_s} = f^{-1}(\mathbf{p_r}) \tag{40}$$

This definition is based on the hypothesis that f is an invertible function.

7 Model data structure

This section will address the representation of the data structures that represent the emitters and receivers, described as above, in order to model the behaviour of a Visible Light Positioning system. For each of these elements, the representation must include:

- the geometric location of the element;
- the parameters that describe the respective behaviour.

Figure 11 presents the data structures for the emitters and receivers, respectively `Emitter_t` and `Receiver_t`. The geometric location is represented by the HTM associated to the element's reference frame and each data structure, for emitters and receivers, contains the remaining parameters that describe the element behaviour.

7.1 Matlab implementation

The data structure defined above allows the representation of a set of emitters or receivers as an array of structures and to compute the optical power detected by the receivers. Referring to the case presented in Section 4, each set of emitters and receivers will be represented by a vector of these structures. Figure 12 depicts the Matlab code to create the emitter and receiver data structures. We

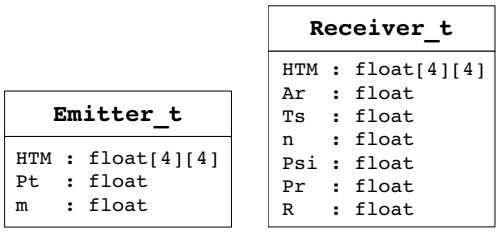

Figure 11: Emitter and receiver data structures

```
%% Create and populate data structures

% Create the emitters array:
Emitters = newEmitters(n_Emitters,Pt, m);

% Create the receiver structure:
Receivers = newReceivers(n_Receivers,Ar, Ts, n, Psi);
```

Figure 12: Matlab code to create data representing emitters and receivers.

consider a system with 3 emitters. The receivers are organized in a hemispherical sensor, where the photo-detectors are placed at the intersection of meridian and parallel lines; there are 5 parallel lines and 6 meridians, yielding a total of 30 receivers. The variables with the sensor parameters where previously defined.

For the purpose of presenting the simulation model, these emitters and receivers are placed in a 3-dimensional space as follows:

- The system is considered to be in a room with dimensions 3mx3mx2m (width, length and height);
- Emitters are placed at the ceiling, the emission axis pointing down and place in a circle of 0.5m radius;
- Receivers are organized in an arrangement of photo detectors, with Nm meridians and Np Parallels, in a hemisphere with radius 0.25m. This sensor is initially place at position $(x, y) = (0.5, 3)$, at ground level.

Figure 13 presents the location of the emitters' and receivers' reference frames, the z axis being plotted in red. We can identify the 3 emitters, located at a height $z = 2$, and the set of receivers in a hemispherical arrangement. The code to generate the corresponding HTM is presented in figure 14. Figure 15 presents the code to generate the plot in Figure 13.

Having defined the emitter and receiver characteristics, as well as their position in space, we are now ready to run the simulation and compute the signal detected by each receiver. The first step is to compute **A**, **B** and **F** matrices (figure 16).

The computation of the received power corresponds to applying (15) using the defined data structures, as shown in figure 17 and assigning the computed values to the receivers' `Pr` attribute.

As an example, we present in Figures 18 and 19 the results for the computation of the received optical power in four different locations, when the sensor is

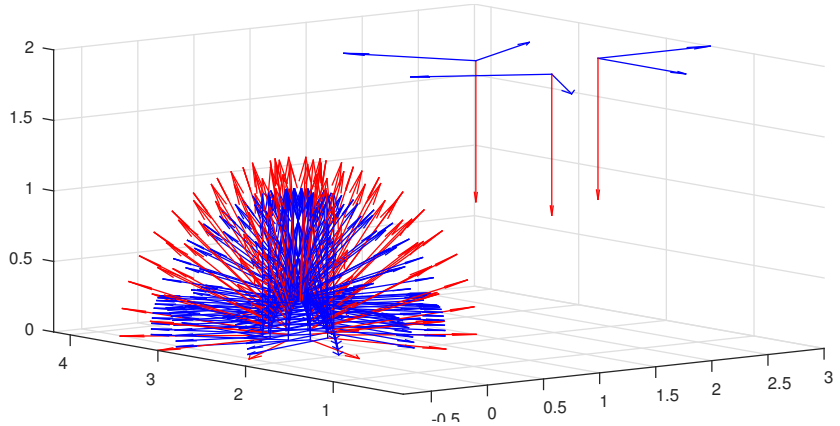

Figure 13: Location of emitters and receivers.

```
% Considering a room with 3mx3mx2m (WxLxH).

% Emitters are placed at the ceiling, looking down
% and in a circle of radius=0.5m

% Base HTM at the center of the ceiling.
Em_Base_HTM = Trans3(1.5,1.5,2)*RotX3(pi);

Emitters(1).HTM = Em_Base_HTM*Trans3(0.5,0,0);
Emitters(2).HTM = Em_Base_HTM*RotZ3(2*pi/3)*Trans3(0.5,0,0);
Emitters(3).HTM = Em_Base_HTM*RotZ3(4*pi/3)*Trans3(0.5,0,0);

% Receivers are organized in Parallel and Meridians arragement of
% photo detectors, with Nm Meridians and 3 Parallels, in a sphere
% with radius=0.25
PDSensor = vlpCreateSensorParMer(Receivers, Np, Nm, 0.25);

% The sensor is initially placed at point (X,Y) = (0.5,3)
PDSensor = vlpMoveSensor(PDSensor,Trans3(0.5,3,0));
```

Figure 14: Code for emitters and receivers positioning in 3D space.

```
figure(1)
PlotHTMArray(Emitters);
PlotHTMArray(PDSensor);
view(3)
axis 'equal'
grid on
% Adjust the point of view
view(-38,8);
```

Figure 15: Code for emitters and receivers 3D location plot.

```
%% Compute A, B and F matrices

A = Receiver2A(Receivers);
B = Emitter2B(Emitters);
F = EmitRec2F(Emitters, Receivers);
```

Figure 16: Computation of **A**, **B** and **F** matrices.

```
%% Compute the received power

Pt_v = [Emitters.Pt]'; % vector with the emitters Pt
Pr = A*F*B*Pt_v


% Update the PDSensor received power
for i=1:numel(PDSensor)
    PDSensor(i).Pr = Pr(i);
end
```

Figure 17: Code for computing the received power.

displaced across the room. In this plot, the received power P_r is represented by the length of a vector aligned with the photo-detector's reference frame z axis. In the first case, the photo-detectors FOV is $\pi/2$, in the second case, $\pi/6$. The effect of narrowing the field-of-view of the sensor detectors is visible. The code for generating these results is presented in figure 20.

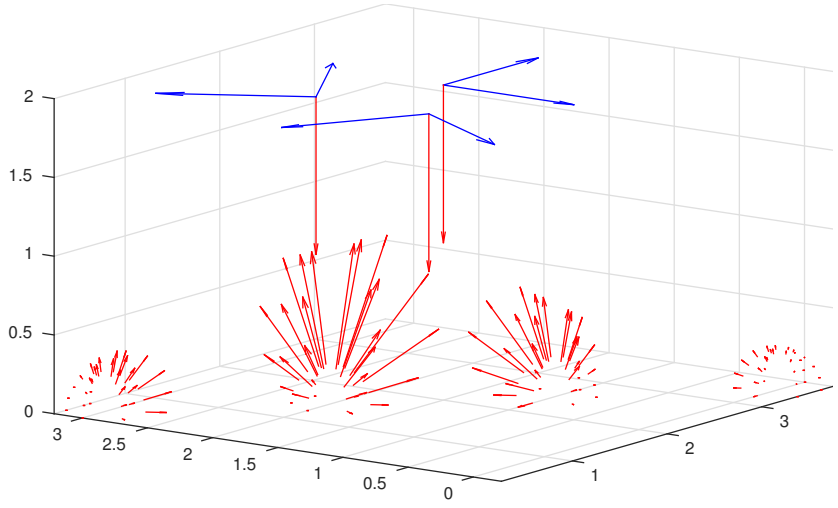

Figure 18: Simulation of a sensor with FOV=$\pi/2$.

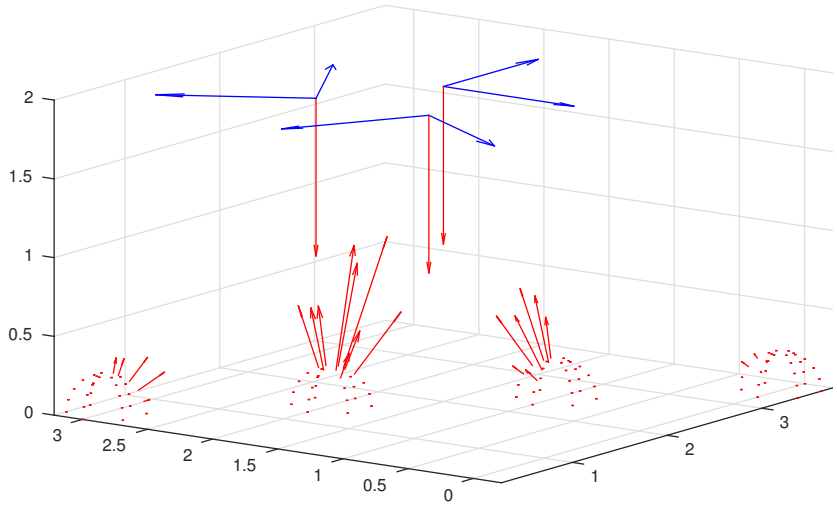

Figure 19: Simulation of a sensor with FOV=$\pi/6$.

```
% Move the sensor, compute new received power and plot received
% power intensity
for i=1:3
    PDSensor = vlpMoveSensor(PDSensor,Trans3(1,-1,0));
    % Recompute the F matrix
    F = EmitRec2F(Emitters, PDSensor);

    % Compute received power
    Pt_v = [Emitters.Pt]';
    Pr = A*F*B*Pt_v;

    % Get the new max valuefor scaling the received power plot
    MaxPr = max(Pr);

    % Update the PDSensor received power
    for i=1:numel(PDSensor)
        PDSensor(i).Pr = Pr(i);
    end

    % Plot the receiver power intensities, scaled
    PlotHTMArrayPr(PDSensor,k*MaxPr/MaxPr0);

end
```

Figure 20: Code for computing the received power when the sensor is displaced.

References

[1] R. P. Paul, *Robot Manipulators — Mathematics, Programming and Control*, ser. The MIT Press Series in Artificial Intelligence. The MIT Press, 1981.

[2] Ziyan Jia, "A Visible Light Communication Based Hybrid Positioning Method for Wireless Sensor Networks," *Intelligent System Design and Engineering Application (ISDEA), 2012 Second International Conference on*, pp. 1367–1370, 2012. [Online]. Available: http://ieeexplore.ieee.org/document/6173463/

[3] J. Armstrong, Y. Sekercioglu, and A. Neild, "Visible light positioning: a roadmap for international standardization," *Communications Magazine, IEEE*, vol. 51, no. 12, pp. 68–73, Dec. 2013. [Online]. Available: http://ieeexplore.ieee.org/document/6685759/

[4] F. Gfeller and U. Bapst, "Wireless in-house data communication via diffuse infrared radiation," *Proceedings of the IEEE*, vol. 67, no. 11, pp. 1474–1486, 1979. [Online]. Available: http://ieeexplore.ieee.org/document/1455777/

[5] J. Kahn and J. Barry, "Wireless infrared communications," *Proceedings of the IEEE*, vol. 85, no. 2, pp. 265–298, Feb. 1997. [Online]. Available: http://ieeexplore.ieee.org/document/554222/

[6] J. Barry, J. Kahn, W. Krause, E. Lee, and D. Messerschmitt, "Simulation of multipath impulse response for indoor wireless optical channels," *IEEE Journal on Selected Areas in Communications*, vol. 11, no. 3, pp. 367–379, Apr. 1993. [Online]. Available: http://ieeexplore.ieee.org/document/219552/

[7] Z. Ghassemlooy, W. Popoola, and S. Rajbhandari, *Optical wireless communications: system and channel modelling with MATLAB*. Boca Raton, Fla.: CRC Press, 2013.

[8] J. Grubor, S. Randel, K.-D. Langer, and J. W. Walewski, "Broadband Information Broadcasting Using LED-Based Interior Lighting," *Journal of Lightwave Technology*, vol. 26, no. 24, pp. 3883–3892, Dec. 2008. [Online]. Available: http://ieeexplore.ieee.org/document/4758667/

[9] L. Zeng, D. O'Brien, H. Le-Minh, K. Lee, D. Jung, and Y. Oh, "Improvement of Date Rate by using Equalization in an Indoor Visible Light Communication System." IEEE, May 2008, pp. 678–682. [Online]. Available: http://ieeexplore.ieee.org/document/4536841/

[10] L. Zeng, D. O'Brien, H. Minh, G. Faulkner, K. Lee, D. Jung, Y. Oh, and E. Won, "High data rate multiple input multiple output (MIMO) optical wireless communications using white led lighting," *IEEE Journal on Selected Areas in Communications*, vol. 27, no. 9, pp. 1654–1662, Dec. 2009. [Online]. Available: http://ieeexplore.ieee.org/document/5342325/

[11] K. Lee and H. Park, "Channel model and modulation schemes for visible light communications." IEEE, Aug. 2011, pp. 1–4. [Online]. Available: http://ieeexplore.ieee.org/document/6026479/

[12] John E. Greivenkamp, *Field guide to geometrical optics*, ser. SPIE field guides. Bellingham, Wash: SPIE Press, 2004, no. v. FG01.

[13] Texas Instruments, "OPA657 1.6-GHz, Low-Noise, FET-Input Operational Amplifier," Texas Instruments, Datasheet, Dec. 2015. [Online]. Available: http://www.ti.com/lit/ds/symlink/opa657.pdf

[14] Walt Kestler, "Op Amp Noise," Analog Devices, Tech. Rep. MT-047, 2009. [Online]. Available: http://www.analog.com/media/en/training-seminars/tutorials/MT-047.pdf